



HAL
open science

Analysis of Operational Amplifier Susceptibility to Multifrequency Disturbance

Alexandre Boyer, Fabrice Caignet

► **To cite this version:**

Alexandre Boyer, Fabrice Caignet. Analysis of Operational Amplifier Susceptibility to Multifrequency Disturbance. 1st International Workshop on the Electromagnetic Compatibility of Integrated Circuits, Oct 2024, Turin (IT), Italy. hal-04734444

HAL Id: hal-04734444

<https://laas.hal.science/hal-04734444v1>

Submitted on 14 Oct 2024

HAL is a multi-disciplinary open access archive for the deposit and dissemination of scientific research documents, whether they are published or not. The documents may come from teaching and research institutions in France or abroad, or from public or private research centers.

L'archive ouverte pluridisciplinaire **HAL**, est destinée au dépôt et à la diffusion de documents scientifiques de niveau recherche, publiés ou non, émanant des établissements d'enseignement et de recherche français ou étrangers, des laboratoires publics ou privés.

Analysis of Operational Amplifier Susceptibility to Multifrequency Disturbance

A. Boyer
 LAAS-CNRS, Univ. de Toulouse, INSA, UPS, LAAS
 Toulouse, France
 alexandre.boyer@laas.fr

F. Caignet
 LAAS-CNRS, Univ. de Toulouse, INSA, UPS, LAAS
 Toulouse, France
 fcaignet@laas.fr

Abstract—This paper deals with the susceptibility of operational amplifiers (op-amps) in multifrequency injection. After an in-depth analysis of the different failure mechanisms that induces DC-offset based on experimental results on a general-purpose op-amp, the paper proposes a risk assessment method based on continuous wave susceptibility test results.

Keywords— susceptibility, operational amplifier, multitone disturbance

I. INTRODUCTION

Operational amplifier (op-amp) is a common circuit in analog functions, such as signal conditioning stage, bandgap reference or linear voltage regulators, but it can be particularly sensitive to RF disturbance. The RF signals can be rectified, leading to EMI-induced offset as described and modelled in numerous scientific books and publications, e.g. [1] [2] [3]. However, most of the research works dealt with continuous wave (CW) disturbance, except [4] where two-tone interference is considered.

However, with the growing complexity of EM environments, questions about the EMI-risk assessment of electronic devices in a real environment arises [5]. A particularly important question is the behaviour of electronic devices to multifrequency or multitone disturbance. Because of the non-linear behaviour of ICs, predicting their response to multifrequency disturbance is not an obvious task. Moreover, testing the susceptibility to multitone EM disturbance can become exponentially long because of the large number of frequency/amplitude/phase combinations.

This paper aims at clarifying the failure mechanisms that leads to EMI-induced offset in general-purpose op-amps submitted to a multifrequency disturbance, through experiments and simulations. In this study, only conducted disturbance applied on the non-inverting pin of the op-amp is considered, as it may be connected to long traces and couple EM disturbance. This paper also proposes a first attempt of a risk assessment method based on CW susceptibility test results to predict the failure threshold of op-amps exposed to multifrequency disturbance. The paper is organized as follows: after a rapid description of the op-amp used as a case study and a brief presentation of its susceptibility to CW disturbance, Section IV analyses the failure mechanisms to multifrequency injection. It highlights the possible links with the CW test results and the limits. Then, a risk assessment method is derived and tested in Section V.

II. PRESENTATION OF THE CASE STUDY AND CW SUSCEPTIBILITY

This study relies on a general-purpose op-amp, the reference LMV651 from Texas Instruments. The RF susceptibility of this IC has been studied in [6]. It exhibits the typical failure mechanisms of op-amps to CW disturbance, so the conclusion drawn from this study could be extended to

other general-purpose op-amps. Moreover, a simplified behavioral model of this op-amp has been proposed in [6] to simulate the two main mechanisms responsible of the EMI-induced offset: slew-rate (SR) asymmetry and weak distortion (WD) of the input differential pair [1].

In this study, the op-amp is mounted in a typical non-inverting configuration. Two 1 k Ω resistors are used for the feedback connection between the output and the non-inverting input, to ensure a sufficient bandwidth and that the maximum output current limit is not exceeded. The conducted susceptibility to RF disturbance applied on the non-inverting input pin (V+) is measured according to the IEC62132-4 Direct Power Injection standard. The experimental set-up is described in Fig. 1. The test equipment is listed in Table I. An arbitrary waveform generator (AWG) is used to produce both the CW and multifrequency disturbance. The test is restricted between 10 MHz and 1 GHz, due to the bandwidth limitations of the AWG. The EMI-induced DC offset is monitored by a precision voltmeter. The amplitude of the conducted disturbance is given in terms of forward voltage or power and is measured by a power meter through a directional coupler. The presence of harmonics and intermodulation products due to the distortion at V+ pin is detected by a spectrum analyzer which monitors the reflected voltage. During all the experiments, no distortion of the disturbance applied on the op-amp input was detected, proving that the input impedance of the non-inverting input remains unchanged. The measurement uncertainty is estimated to less than 1 dB.

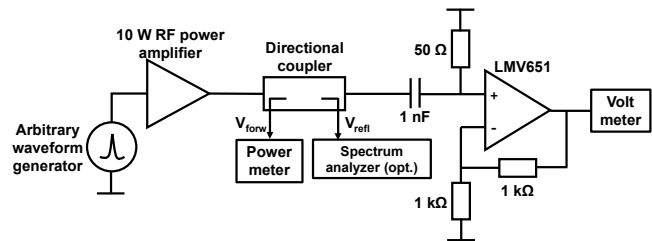


Fig. 1. Experimental set-up.

TABLE I. LIST OF TEST EQUIPMENTS

| Equipment | Reference |
|---------------------|-----------------------------|
| AWG | Tektronix AWG710B |
| RF power amplifier | Amplifier Research 10W1000B |
| Power Meter | R&S NRVD |
| Directional Coupler | HP 778D |
| Spectrum Analyzer | Anritsu MS2667C |
| Voltmeter | Agilen 34405A |

Initially, the susceptibility of the LMV651 to CW disturbance is tested. The AWG is configured to produce a sine waveform. Fig. 2 presents the susceptibility threshold of the op-amp measured for different values of EMI-induced offset (5, 10 20 and 40 mV). The sign of the offset is also depicted on the graph. Up to 100 MHz, the EMI-induced

offset is due to the SR rate asymmetry. Due to a larger positive slew-rate, a positive offset is induced. Each time the offset is doubled, the required forward power is increased by 3 to 4 dB. Above 100 MHz, the EMI-induced offset becomes negative and is due to the WD of the differential pair. The gap between the curves is about 3 dB, showing also that the offset does not follow a linear relationship according to the applied voltage. Between 80 and 150 MHz, the influence of SR asymmetry tends to be compensated by the WD influence which becomes dominant. The compensation is clearly visible in this range, where a corner frequency appears with a large increase of the immunity level. This corner frequency changes according to the maximum offset limit, as it changes the conditions of an exact compensation.

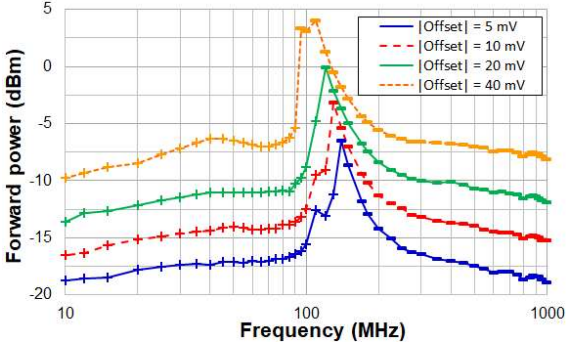


Fig. 2. Susceptibility threshold of the tested op-amp to CW disturbance. '+' means a positive offset and '-' a negative offset.

III. FAILURE MECHANISMS IN MULTIFREQUENCY INJECTION

In this section, the influence of the different failure mechanisms on the EMI-induced offset is analyzed in the case of a multifrequency injection. Here, only two-tone injection is considered for clarification purpose.

A. Weak-Distortion of the Differential Pair

The EMI-induced offset due to the WD of the differential pair has been extensively used in previous researches, as this mechanism usually dominates above 100 MHz. Closed-form expressions of the offset have been derived, such as [2], showing that the offset at a frequency ω_i depends on the square of the applied voltage on the non-inverting input V^+ , as suggested by (1) and (2). H is a transfer function that depends on the op-amp and its configuration and \bar{X} refers to the average value of X . This trend is confirmed by the experimental result measured on LMV651 output.

$$V_{off}(\omega_i) = \overline{H(\omega_i)V^+(\omega_i)^2} = \overline{H(\omega_i)A_i^2 \cos(\omega_i t + \phi_i)^2} \quad (1)$$

$$V_{off}(\omega_i) = H(\omega_i) \frac{A_i^2}{2} \quad (2)$$

As suspected in [4], this type of relationship leads to a relatively simple behavior in multifrequency injection. Let consider a multifrequency disturbance composed of N tones with different frequencies ω_i , amplitude A_i and phase ϕ_i . The offset is given by (3), which is actually the sum of the individual contribution of each tone without any influence of their phase. The offset is related to the average power of each tone.

$$V_{off} = \overline{\sum_{i=1}^N H(\omega_i)A_i^2 \cos(\omega_i t + \phi_i)^2} = \sum_{i=1}^N H(\omega_i) \frac{A_i^2}{2} \quad (3)$$

In order to verify this property, a two-tone injection test is made with frequencies $F_1 = 300$ MHz and $F_2 = 319$ MHz. The amplitude of the first harmonic V_{forw1} is kept constant, while the amplitude of the second one V_{forw2} is increased. The evolution of the offset according to V_{forw2} , for two different values of V_{forw1} , is plotted in Fig. 3. The theoretical offset is also computed as the sum of the measured offset in CW tests. A good agreement is observed up to an offset of -40 mV, proving that the contributions of both harmonics sum together. This property is also verified for a larger number of tones.

B. Slew-Rate Asymmetry

As reported in numerous research publications, the EMI-induced offset up to several tens of MHz is essentially due to the unavoidable SR asymmetry. Although this phenomenon is well-known, it remains a strong linear distortion which resists to closed-form expressions. In CW injection, Fig. 4 shows the evolution of the EMI-induced offset measured according to the disturbance amplitude at three different frequencies where the influence of SR asymmetry dominates. Contrary to the WD, the trend is less clear. As long as the amplitude of the disturbance remains low, the offset tends to increase according to a quadratic evolution. The error with the quadratic model is less than 10 % when the offset does not exceed 20 to 25 mV. Then, the offset increase slows down and tends to a linear evolution for medium amplitude of the disturbance. This type of evolution is confirmed by simulations based on the behavioral model developed in [6]. For larger amplitude, the positive offset tends to be compensated by the influence of the WD.

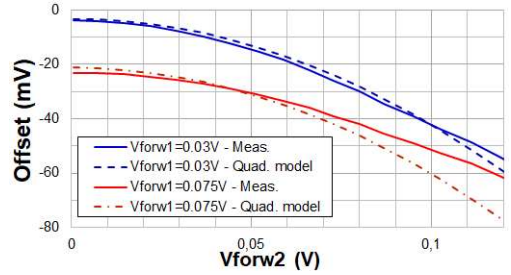


Fig. 3. Evolution of the offset in a two-tone injection test when the WD failure mechanism dominates ($F_1 = 300$ MHz and $F_2 = 319$ MHz).

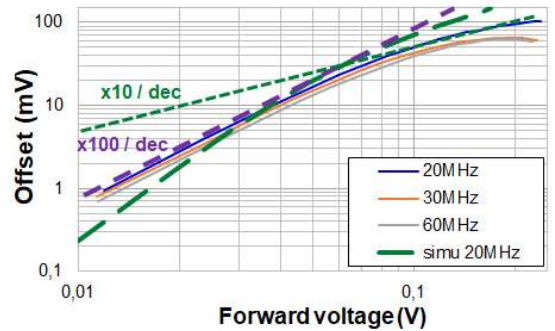


Fig. 4. Measured evolution of the EMI-induced offset when the slew rate asymmetry mechanism dominates.

A two-tone injection test is made on the op-amp with frequencies ranging from 10 to 100 MHz. Fig. 5 presents the evolution of the measured offset according to V_{forw2} for a constant amplitude V_{forw1} , with $F_1 = 20$ MHz, $F_2 = 29$ MHz and identical phase (changing the phase has actually no effect on the induced offset). The evolution of the offset in CW injection at F_2 is also reported. It appears that the resulting offset is not the sum of the individual contribution of each

tone. Moreover, adding a second tone contributes to reduce the offset compared to CW injection, especially if both tones have similar amplitudes. This effect is also observed in simulation.

These results reveal the complex non-linear behavior of the SR asymmetry mechanism. In a first approximation, for small offset value, (4) is proposed to combine the influence of the different tones on the SR. It provides a reasonably good estimation of the offset in the case of a two-tone injection, as shown by Fig. 6, where the error does not 20 % for a maximum offset of 40 mV.

$$V_{off} = \sqrt{\sum_{i=1}^N V_{off}(\omega_i)^2} \quad (4)$$

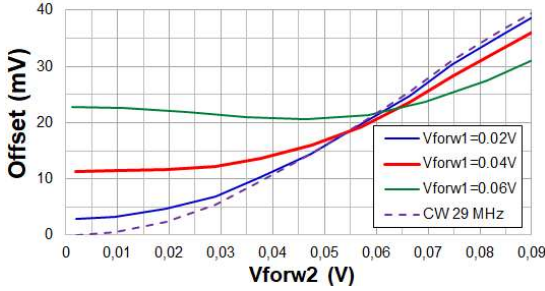


Fig. 5. Evolution of the measured offset in a two-tone injection test, the SR asymmetry failure mechanism dominates ($F_1 = 20$ MHz and $F_2 = 29$ MHz).

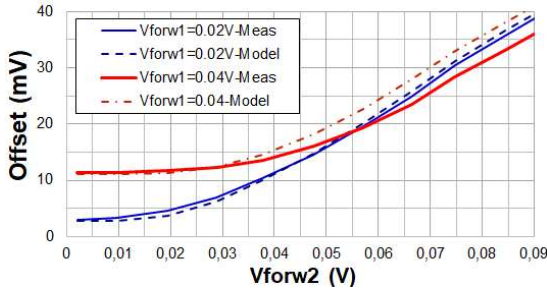


Fig. 6. Comparison between measured and predicted EMI-induced offset with the combination model (4) of the influence of the different tones ($F_1 = 20$ MHz and $F_2 = 29$ MHz).

IV. EVALUATION OF THE RISK OF FAILURE DUE TO EMI-INDUCED OFFSET IN MULTIFREQUENCY INJECTION

A. Description of the method

The previous section proves that the exact computation of the EMI-induced offset in multifrequency injection is not an obvious task because of the non-linear behavior of op-amp and the simultaneous existence of several failure mechanisms. The failure assessment in multifrequency injection can become a complex and tedious task if the susceptibility of the op-amp has to be tested with a large number of combinations of frequency, amplitude and phase. However, different observations can be used to determine the risk of EMI-induced offset failure from the CW susceptibility test results, especially for small to medium offset values (less than several tens of mV) which correspond to usual failure criterion level in typical analog functions.

Firstly, let consider the offset due to WD mechanism. (3) shows that the offset is the sum of the offset produced individually by each tone and depends on the average power of the tone. This property leads to a simple correlation between CW and multifrequency susceptibility levels when

the failure results from the linear superposition of the contribution of each injected harmonic [7]. If the electronic device is submitted to multifrequency disturbances composed of M harmonics with frequencies f_k and average power P_{Ek} , $k \in [1; M]$, failure arises if (5) is verified. P_{Sk} is the susceptibility threshold of the DUT to CW disturbance measured at a frequency f_k and I_{tot} is the interference coefficient. The impact of each harmonic is weighted by the CW susceptibility threshold in order to account for the susceptibility of the DUT at frequency f_k . When the sum of the weighted harmonics exceeds 1, the failure arises.

$$I_{totWD} = \sum_{k=1}^M \frac{P_{Ek}}{P_{Sk}} = 1 \quad (5)$$

Secondly, for the offset due to SR asymmetry, the offset increases with the applied voltage according to a quadratic relationship in CW injection if the offset does not exceed several tens of mV. Thus, it depends on the average power of the applied CW disturbance. Moreover, the offset in multifrequency injection can be approximated as the square root of the sum of square of the offset due to each applied tone (4). Therefore, (5) can be rewritten for the case of SR and the interference coefficient I_{totSR} can be defined by (6), where $offset_{meas}$ is the offset measured in the tested multifrequency injection scenario and $offset_{max}$ is the maximum allowed offset defined for the susceptibility test.

$$I_{totSR} = \frac{offset_{meas}}{offset_{max}} = \sqrt{\sum_{k=1}^M \left(\frac{P_{Ek}}{P_{Sk}} \right)^2} \quad (6)$$

From the CW susceptibility test results obtained for a given definition of the maximum offset, (5) and (6) offer a simple method to determine whether a combination of M tones may lead to a failure (offset > $offset_{max}$). This situation may happen if I_{tot} exceeds 1. These formulas may be used only if all the tones activate either the WD mechanism (5) or the SR asymmetry (6). In the case where M_1 tones activate the WD mechanism and M_2 tones the SR asymmetry, the offset due to both mechanisms adds together and (7) can be used to determine the interference coefficient, where $sign_{WD}$ and $sign_{SR}$ give the offset due to WD and SR respectively.

$$I_{tot} = sign_{WD} \sum_{k=1}^{M_1} \frac{P_{Ek}}{P_{Sk}} + sign_{SR} \sqrt{\sum_{k=1}^{M_2} \left(\frac{P_{Ek}}{P_{Sk}} \right)^2} \quad (7)$$

B. Validation

In order to validate the failure assessment method, three and four tones tests are made to verify that the failure triggering is detected correctly when the amplitude of the simultaneously-injected tones is changes. Two limits for the maximum offset are considered: ± 10 and ± 20 mV. For each test, combinations of three or four frequencies (F_1, F_2, F_3, F_4) are selected randomly with different amplitudes also chosen randomly. The amplitudes, written V_1, V_2, V_3, V_4 , are expressed in forward voltage. Phases are identical as experimental results show that the phase has no significant influence. For three-tone injection test, the amplitude V_3 of the third harmonic is increased while the two others are kept constant. Similarly, for four-tone injection test, the amplitude V_4 of the fourth harmonic is increased. For each tested amplitude of V_3 or V_4 , I_{tot} is computed according to (7), from the CW susceptibility thresholds given in Fig. 2, and the op-

amp offset is monitored. The evolutions of I_{tot} and the offset for the different tested scenarios are compared in order to verify that I_{tot} is equal to 1 when the offset limit (10 or 20 mV) is reached.

Figs. 7 to 12 present the experimental results for the different tested scenarios, with different couples of frequencies, amplitudes and offset limits. In Figs 7 and 8, the

injected frequencies range between 200 and 1000 MHz in order to activate only the WD mechanism. In Figs 9 and 10, the injected frequencies are limited to the range 10 to 100 MHz and only the failure related to the SR asymmetry is activated. In Figs 11 and 12, the injected frequencies are selected between 10 and 1000 MHz to activate simultaneously both failure mechanisms.

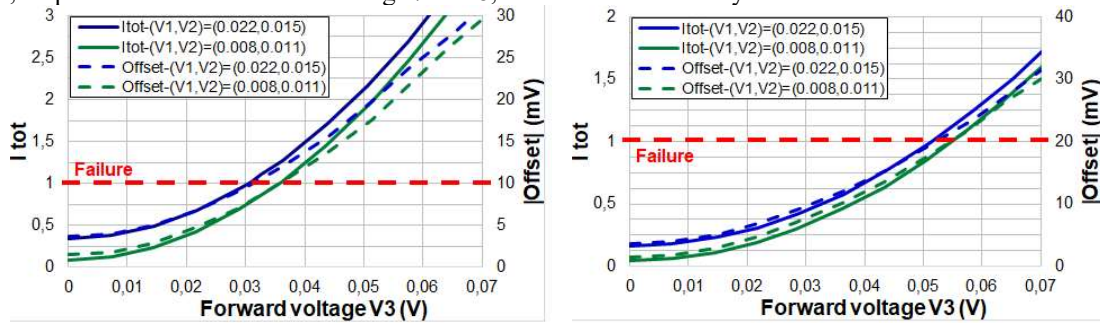


Fig. 7. Risk assessment when the WD dominates for a maximum EMI-induced offset of 10 mV (left) and 20 mV (right) for three-tone injection: $F_1 = 271$ MHz, $F_2 = 336$ MHz, $F_3 = 802$ MHz.

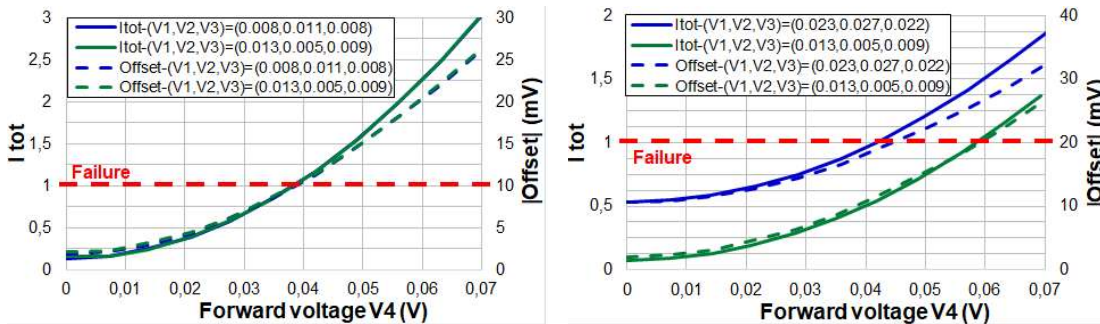


Fig. 8. Risk assessment when the WD dominates for a maximum EMI-induced offset of 10 mV (left) and 20 mV (right) for four-tone injection: $F_1 = 271$ MHz, $F_2 = 336$ MHz, $F_3 = 802$ MHz, $F_4 = 559$ MHz.

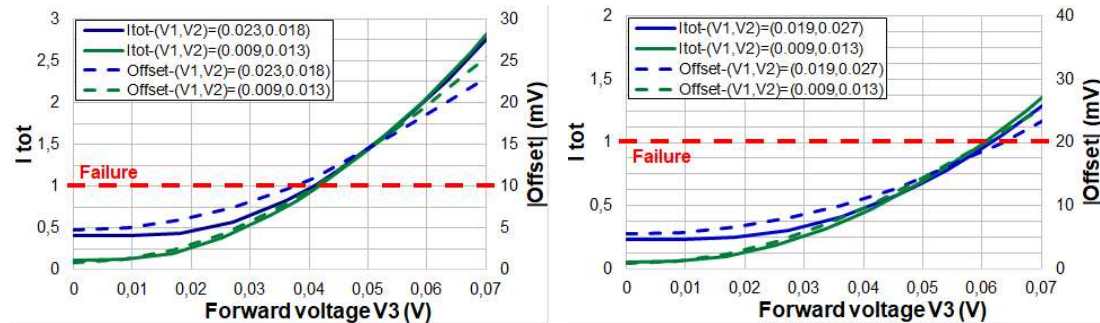


Fig. 9. Risk assessment when the SR asymmetry dominates for a maximum EMI-induced offset of 10 mV (left) and 20 mV (right) for three-tone injection: $F_1 = 23$ MHz, $F_2 = 49$ MHz, $F_3 = 81$ MHz.

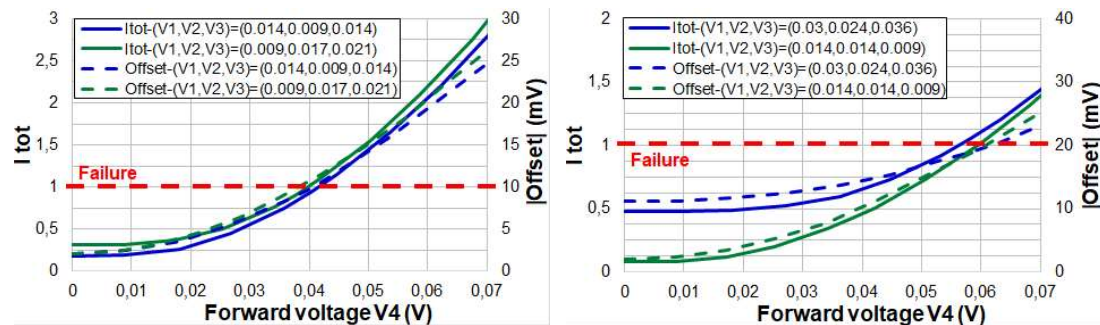


Fig. 10. Risk assessment when the SR asymmetry dominates for a maximum EMI-induced offset of 10 mV (left) and 20 mV (right) for four-tone injection: $F_1 = 23$ MHz, $F_2 = 49$ MHz, $F_3 = 81$ MHz, $F_4 = 57$ MHz.

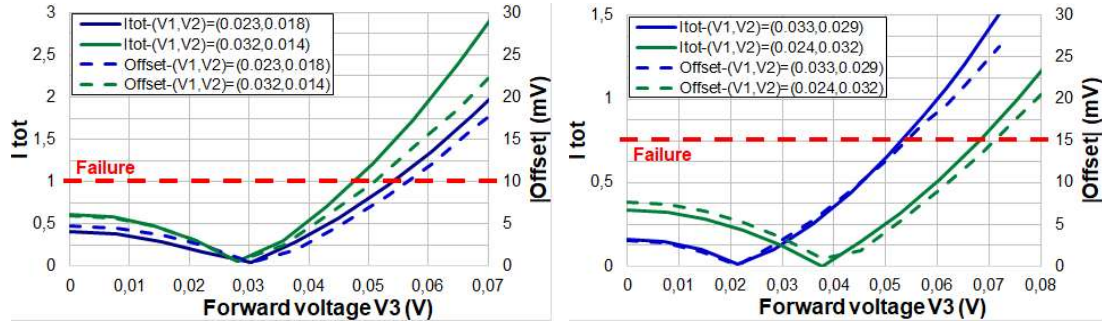


Fig. 11. Risk assessment with both failure mechanisms for a maximum EMI-induced offset of 10 mV (left) and 20 mV (right) for three-tone injection: $F_1 = 23$ MHz, $F_2 = 49$ MHz, $F_3 = 316$ MHz.

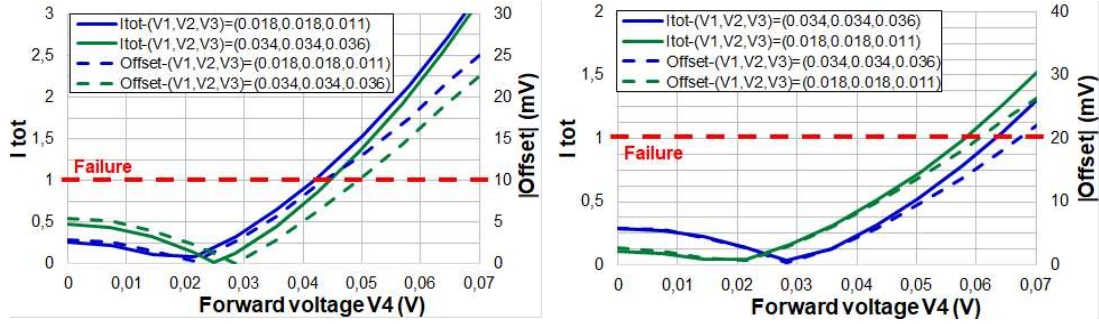


Fig. 12. Risk assessment with both failure mechanisms for a maximum EMI-induced offset of 10 mV (left) and 20 mV (right) for four-tone injection: $F_1 = 23$ MHz, $F_2 = 49$ MHz, $F_3 = 316$ MHz, $F_4 = 802$ MHz.

When only one failure mechanism is activated (Figs 7 to 10), the offset increases continuously with the disturbance amplitude and the indicator I_{tot} crosses the limit 1 when the offset reaches the failure threshold. It is reached more or less rapidly according to the selection of V_1, V_2, V_3, V_4 values. The results show that there is a good agreement between the evolution of I_{tot} and the offset, especially closed to the failure threshold. For injection made between 200 and 1000 MHz, the difference between the measured susceptibility threshold and the limit given by $I_{tot} = 1$ does not exceed 5 %, i.e. an error less than 0.4 dB. For injection made between 10 and 100 MHz, this difference does not exceed 10 %, i.e. an error less than 1 dB. The difference is explained by the measurement uncertainties and the approximation of the offset evolution models (3) and (4). When both failure mechanisms are activated (Figs. 11 and 12), the offset tends to decrease initially because of the compensation of the opposite effects of WD and SR asymmetry. Then, the WD dominates and the offset increases continuously. A good agreement is also observed between the evolution of I_{tot} and the measured offset. The difference between the measured susceptibility threshold and the limit given by $I_{tot} = 1$ does not exceed 8 %, i.e. an error less than 0.7 dB.

These results show that I_{tot} determines the triggering of op-amp failure, especially when only WD mechanism is activated. The precision is degraded when SR asymmetry is activated, due to the complex evolution of the induced offset as shown in Section III.B. It is also degraded when both failure mechanisms are activated. However, the error remains less than 1 dB, which makes I_{tot} a practically-reliable indicator for multitone susceptibility evaluation.

C. EMI Risk Assessment

In order to evaluate the relevance of the EMI risk assessment, the tested op-amp is submitted to four-tone injection with randomly-selected frequency and amplitudes. The frequencies are selected in the range 10 to 1000 MHz and the normalized amplitudes are comprised between 0 and 1. Two offset limits are considered: ± 10 and ± 20 mV. For each test, the amplitude of the disturbance is increased until the EMI-induced reaches the limit and the indicator I_{tot} is computed based on (7). For each test, 80 samples are randomly drawn. The result of the tests is presented in Fig 13, as an histogram depicting the distribution of I_{tot} when the op-amp failure arises.

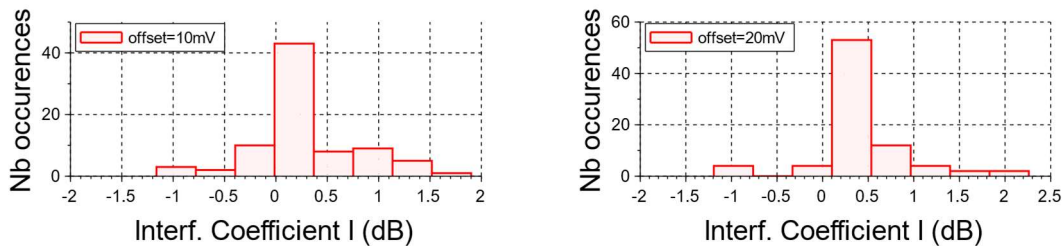


Fig. 13. Risk assessment for four tone injection with randomly-selected frequencies and amplitudes: EMI-induced offset = 10 mV(top), EMI-induced offset = 20 mV(bottom)

Failures arise when I_{tot} ranges between -1 and +1 dB for 70 samples. The average and standard deviation are equal to 0.29 and 0.52 dB for the offset limit of 10 mV, and 0.39 and 0.52 dB for 20 mV. The maximum error reaches 1.9 and 2.2 dB for 10 and 20 mV offset values. A part of the error can be explained by the measurement uncertainty. It can be also explained by the approximation of the used model to evaluate I_{tot} . Most of the samples with $I_{\text{tot}} < -1$ dB are associated to cases where the SR asymmetry dominates. Oppositely, the samples with $I_{\text{tot}} > 1$ dB appear when tones with comparable amplitude fall below 100 MHz and above 200 MHz are injected simultaneously, leading to a compensation of their effect on the offset. In these particular situations, the proposed approach becomes less precise. In spite of that, the indicator I_{tot} succeeds in giving a correct evaluation of the risk of failure in a majority of cases.

V. CONCLUSION

This paper has presented an in-depth analysis of the failure mechanisms responsible of EMI-induced offset in an op-amp submitted to multifrequency injection. In spite of the non-linear behaviour of op-amps, the paper has determined general trends in the evolution of the offset according to the disturbance amplitude and in the combination of the different injected tones for small offset values. From these results, a method has been proposed to determine if an op-amp exposed to a given combination of tones may reach the failure limit. As the approach relies only on CW susceptibility test results, it provides a simple and practical method to estimate the risk of failure in multifrequency injection. The obtained results

have been extracted from experiments done on a general-purpose op-amp and confirmed by simulations on a general behavioural model. An evaluation of the EMI-risk assessment on an op-amp to three and four-tones disturbance has also been done, showing a good agreement with measurement result in most of the tested cases. The accuracy is excellent when the WD mechanism dominates, but it may degrade when SR asymmetry dominates or when both failure mechanisms tend to compensate each other. As a perspective, a deeper analysis and a better modelling of the SR asymmetry would be necessary to improve the accuracy. Moreover, the results should be certainly extrapolated to other op-amps, which will be confirmed in future studies.

REFERENCES

- [1] J. M. Redouté, M. Steyaert, *EMC of Analog Integrated Circuits*, Springer, 2010.
- [2] F. Fiori, "A New Nonlinear Model of EMI-Induced Distortion Phenomena in Feedback CMOS Operational Amplifiers", *IEEE Trans on EMC*, vol. 44, no 4, pp. 495-502, Nov. 2002.
- [3] A. Richelli, "EMI Susceptibility Issue in Analog Front-End for Sensor Applications - Review article", *Journal of Sensors*, 2016.
- [4] F. Fiori, M. Brignone Aimonetto, "Measurement of the Susceptibility to EMI of ICs with Two-Tone Interference", in *Proc. of APEMC 2018*, pp. 292 – 296, Singapore, May 2018.
- [5] D. Pissoort, K. Armstrong, "Why is the IEEE developing a standard on managing risks due to EM disturbances?", in *Proc. of IEEE Int. Symp. on EMC*, pp. 78-83, Ottawa, Canada, Sep. 2016.
- [6] A. Boyer, E. Sicard, "A Case Study to apprehend RF Susceptibility of Operational Amplifiers", *12th Int. Workshop on the EMC of Integrated Circuits (EMC Compo 2019)*, Hangzhou, China, Oct. 21-23 2019.
- [7] A. Boyer, F. Caignet, "A Pre-Scan Method to Accelerate Near-Field Scan Immunity Tests", *IEEE Lett. on EMC Practice and Applications*, Early Access, Feb. 2024, 10.1109/LEMCPA.2024.3363113.